

Mixed-Charge Nanoparticles for Long Circulation, Low Reticuloendothelial System Clearance, and High Tumor Accumulation

Xiangsheng Liu, Huan Li, Yangjun Chen, Qiao Jin, Kefeng Ren, and Jian Ji*

Mixed-charge zwitterionic surface modification shows great potential as a simple strategy to fabricate nanoparticle (NP) surfaces that are nonfouling. Here, the *in vivo* fate of 16 nm mixed-charge gold nanoparticles (AuNPs) is investigated, coated with mixed quaternary ammonium and sulfonic groups. The results show that mixed-charge AuNPs have a much longer blood half-life (≈ 30.6 h) than do poly(ethylene glycol) (PEG, $M_w = 2000$) -coated AuNPs (≈ 6.65 h) and they accumulate in the liver and spleen far less than do the PEGylated AuNPs. Using transmission electron microscopy, it is further confirmed that the mixed-charge AuNPs have much lower uptake and different existing states in liver Kupffer cells and spleen macrophages one month after injection compared with the PEGylated AuNPs. Moreover, these mixed-charge AuNPs do not cause appreciable toxicity at this tested dose to mice in a period of 1 month as evidenced by histological examinations. Importantly, the mixed-charge AuNPs have higher accumulation and slower clearance in tumors than do PEGylated AuNPs for times of 24–72 h. Results from this work show promise for effectively designing tumor-targeting NPs that can minimize reticuloendothelial system clearance and circulate for long periods by using a simple mixed-charge strategy.

1. Introduction

Using nanoparticles (NPs) in biomedicine has brought new hope for cancer diagnosis and treatment.^[1–4] Inorganic NPs such as gold nanoparticles (AuNPs) provide promising tools for biomedical applications including drug and gene delivery, biosensing, bioimaging, and photothermal therapy.^[5–7] However, using them successfully in complex biological systems is not easy.^[8–10] As the enhanced permeability and retention effect has served as a primary rationale for using NPs to treat solid tumors, long-circulating NPs called “stealth nanoparticles” are highly desirable in nanomedicine.^[11,12] Systemically administered NPs should remain in circulation for a long

time to increase their chance of accumulating into disease sites. However, most NPs are easily cleared out from blood by the reticuloendothelial system (RES) or the mononuclear phagocytic system because of non-specific adsorption of proteins.^[11–14] Although PEGylation is an effective and the preferred method for avoiding clearance of NPs by the RES and prolonging the blood half-life of NPs,^[15–19] the poly(ethylene glycol) (PEG) coating has been reported to have disadvantages for *in vivo* applications,^[20] such as accelerated blood clearance after administering a second dose, caused by the development of anti-PEG antibodies by the immune system,^[21,22] and potential *in vivo* degradation through oxidation.^[23] Zwitterionic surfaces provide an alternative means of fabricating stealth surfaces because of their superior nonfouling properties.^[24,25] Recently, modifying NPs, especially inorganic ones, with zwitterionic ligands, has attracted tremendous attention.^[26] Reports

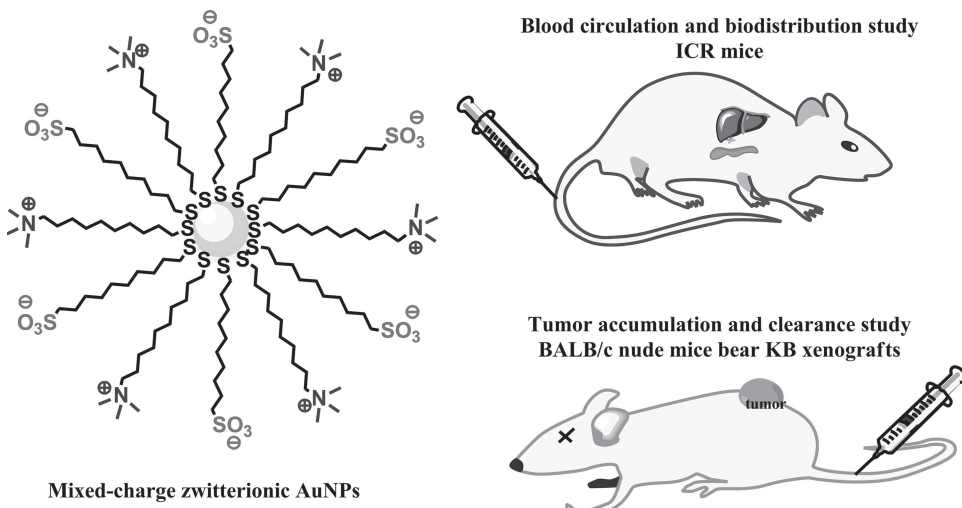
have demonstrated that the zwitterionic surfaces endow NPs with excellent stability and nonfouling properties,^[27–35] and that NPs with zwitterionic surfaces show promise for *in vivo* application.^[36,37]

Instead of using single-component zwitterionic species bearing both a positive and a negative charge in the same molecule to fabricate nonfouling surfaces, the alternative “mixed-charge zwitterionic strategy” using a combination of opposite charges in near-equal amounts on the same surface shows great potential.^[38–44] From a materials scope, the mixed-charge zwitterionic strategy provides many advantages, including simple synthesis, ease of applicability, and an abundance of raw materials from a variety of positively and negatively charged compounds.^[40] Recently, the facile mixed-charge strategy has been successfully applied to stabilize inorganic NPs.^[45–48] Basing on mixed-charge concept, we fabricated stable AuNPs by using mixed-charge self-assembled monolayers (SAMs) with a combination of positive trimethylammonium groups and negative sulfonic groups.^[45] These AuNPs had excellent resistance to non-specific protein adsorption and phagocytosis by macrophages *in vitro*.^[49] Bonitatibus et al.^[46] applied a similar strategy of using mixed organosilanes to form a zwitterionic siloxane polymer coating on the surface of sub-5 nm tantalum oxide NPs. Their

X. S. Liu, H. Li, Y. J. Chen, Dr. Q. Jin,
Dr. K. F. Ren, Prof. J. Ji
MOE Key Laboratory of Macromolecular Synthesis
and Functionalization
Department of Polymer Science and Engineering
Zhejiang University
Hangzhou 310027, China
E-mail: jijian@zju.edu.cn



DOI: 10.1002/adhm.201300617



Scheme 1. Schematics of mixed-charge zwitterionic 16 nm gold nanoparticles (AuNP-C10-SN4), and in vivo animal models used in this study (not to scale).

results showed that the mixed-charge siloxane polymer coating significantly decreased tissue retention of these small particles and did not induce pathological responses in the kidneys.

However, in vivo studies of mixed-charge-modified NPs are still immature. For further developing the application of the mixed-charge NPs in biomedical application, it is important to better understand the in vivo fate of mixed-charge NPs. In this work, we systematically investigated the in vivo behaviors of 16 nm AuNPs coated with a mixed-charge zwitterionic SAM (Scheme 1). Blood circulation of the AuNPs was evaluated by testing the gold content in blood using inductively coupled plasma mass spectrum (ICP-MS). The biodistribution of AuNPs in main organs was investigated up to 1 month by ICP-MS and the intracellular distribution of the AuNPs in the liver and spleen was studied using transmission electron microscopy (TEM). The biocompatibility of mixed-charge AuNPs was evaluated by histological examinations and daily observations. In addition, the accumulation and clearance of AuNPs in tumor tissue were evaluated in xenograft tumors in BALB/c nude mice for times of 24–72 h.

2. Results and Discussion

2.1. Blood Kinetics of Mixed-Charge AuNPs

Mixed-charge zwitterionic AuNPs coated with a combination of trimethylammonium groups and sulfonic groups (AuNP-C10-SN4) and PEG ($M_w = 2000$)-modified AuNPs (AuNP-PEG2000) with the same AuNP core diameter of ≈ 16 nm were prepared as previously reported.^[45] First, we investigated the kinetics of AuNP circulation in the blood stream after intravenously injecting AuNPs into normal Institute of Cancer Research (ICR) mice. The blood circulation curves of the two AuNPs are shown in Figure 1a (given in % injected dose (%ID), and given in %ID/g blood, see Figure S1a and Table S1, Supporting Information). The experimental data can be fitted to a monoexponential decay model,^[18] resulting in a

half-decay time ($t_{1/2}$) of $\approx 30.6 \pm 5.83$ h for the zwitterionic AuNPs and $\approx 6.65 \pm 0.24$ h for the PEGylated AuNPs. The results of AuNP-PEG2000 agreed well with that of similarly sized AuNPs coated with methoxypoly(ethylene glycol) of the same molecular weight.^[50] The half-life of AuNP-C10-SN4 is comparable to that of similarly sized AuNPs coated with PEG with a molecular weight of 5000 Da.^[50,51] Nevertheless, PEG-based ligands with high molecular weight will inevitably increase overly the hydrodynamic diameter of the NPs,^[32,45,50] which is not suitable for designing the NPs with strict requirement of small sizes such as renally clearable NPs.^[52,53] In vivo fate of NPs depends on both their size and surface chemistry. To minimize the interference of size effect, PEG with a smaller molecular weight of 2000 Da was chosen as a control in this research. A long-circulation time in vivo is a combined result of the NPs having low clearance out of the body and strong resistance to the intrinsic defense system of the body.^[54,55] It is thought that NPs should have final hydrodynamic diameters < 5.5 nm to be excreted from the rat body by the renal route.^[52] Since the AuNPs studied in this paper (core size ≈ 16 nm) are larger than this renal filtration cutoff, they may not be excreted in urine. Instead, the elimination of NPs from the blood by the RES will be the main factor affecting the final blood circulation time. Once NPs enter the bloodstream, they are susceptible to nonspecific plasma protein adsorption, known as opsonization.^[12,14] The opsonized NPs can be easily captured by the RES, mainly located in the liver and spleen, which clears the NPs from blood circulation. The long blood half-life of the mixed-charge AuNPs can be considered to be mainly caused by their zwitterionic surface, which have excellent resistance to nonspecific plasma protein adsorption^[45] and uptake by the cells in the RES such as macrophages.^[49] These results strongly indicate that the mixed-charge strategy can be used to effectively design long-circulating NPs.

2.2. Behavior of Mixed-Charge AuNPs in Main Organs

Next, we studied the biodistribution of mixed-charge AuNPs in ICR mice for a period up to 1 month after a single injection.

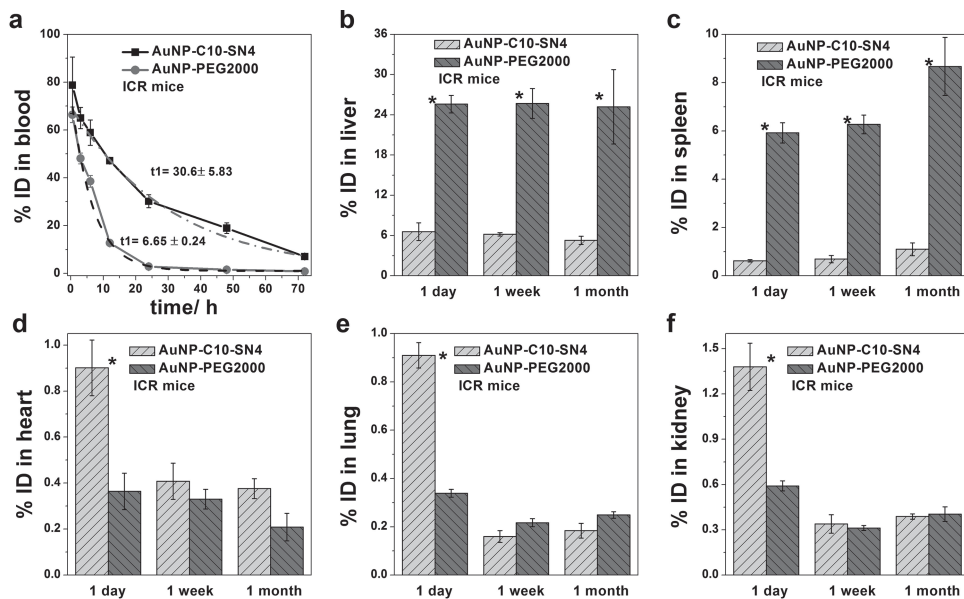


Figure 1. Blood kinetics and biodistribution of mixed-charge and PEGylated AuNPs in male ICR mice. a) The blood circulation curves of AuNP-C10-SN4 and AuNP-PEG2000. The circulation half-lives of AuNPs were fitted to a monoexponential decay model. b–f) Biodistribution of AuNP-C10-SN4 and AuNP-PEG2000 in main organs including liver (b), spleen (c), kidney (d), heart (e), and lung (f) at 1 d, 1 week, and 1 month postinjection (p.i.) at dose of 100 μ g Au per mouse. Each group contained three animals, and results are shown as mean \pm S.D., asterisk indicates significant difference, * $p < 0.05$.

First, we considered the accumulation of AuNPs in the liver and spleen (representative RES organs). The accumulation of AuNP-C10-SN4 in the liver was much lower than that of AuNP-PEG2000 at 24 h postinjection (p.i.), where the content of AuNP-C10-SN4 was about three times lower than that of AuNP-PEG2000 ($\sim 6.6\%$ ID vs $\sim 25.6\%$ ID, Figure 1b). The difference in spleen accumulation between the two AuNPs became more significant, where the content of AuNP-C10-SN4 was about seven times lower than that of AuNP-PEG2000 at 24 h p.i. ($\sim 0.62\%$ ID vs $\sim 5.92\%$ ID, Figure 1c). The spleen is the most important filter of the body and smaller NPs can better avoid splenic filtration.^[55] The AuNP-C10-SN4 particles capped by small molecular ligands have smaller hydrodynamic diameters than the AuNP-PEG2000 particles; this smaller diameter predisposes them toward splenic escape. The hydrodynamic sizes of the AuNPs as detected in phosphate buffered saline (PBS) and serum were ~ 17 nm and ~ 20 nm for AuNP-C10-SN4, while they were ~ 31 nm and ~ 38 nm for AuNP-PEG2000 (Figure S2, Supporting Information). The small difference between PBS and serum might be due to slight protein adsorption of the NPs into the serum; besides, the presence of serum somewhat affected the measured results. The values of both AuNPs are much smaller than the specific filtration cutoff of ~ 100 nm for sinusoids in the spleen,^[9,10] and the difference between the two AuNPs is less than 20 nm, which cannot explain their significant difference in splenic accumulation.^[50] The zeta potential of AuNPs in PBS was measured by DLS measurements, and the values were -9.8 ± 0.5 mV and -10.5 ± 2.5 mV for mixed charge AuNPs and AuNP-PEG2000, respectively. The surface of mixed charge AuNPs is a mixture of positively and negatively charged groups and the surface of AuNP-PEG2000 is neutral ethylene glycol segments, although the surface chemistry is quite different between mixed charge AuNPs and AuNP-PEG2000, both

AuNPs demonstrate similar zeta potential, which is slightly negative. These results also indicated that the different in vivo behaviors between mixed charge AuNPs and AuNP-PEG2000 was mainly resulted from the surface chemistry rather than the overall surface charge. Therefore, we believe that the mixed-charge surface, which endowed the AuNPs with zwitterionic property for strong protein resistance, is the main reason for the extremely low accumulation of AuNP-C10-SN4 in the spleen, as they would be able to effectively escape phagocytosis by macrophages in the spleen.^[55] The low uptake of AuNP-C10-SN4 in the liver can also be accounted for by this surface effect, which provided the AuNPs with excellent antifouling property. In addition, considering that the liver is much larger than the spleen, the concentration of AuNP-PEG2000 in the spleen was more than twice that in the liver ($\sim 43.9\%$ ID/g vs $\sim 18.9\%$ ID/g, and given in%ID/g tissue, see Figure S1b,c, Supporting Information) but both concentrations of AuNP-C10-SN4 were similarly low ($\sim 4.6\%$ ID/g liver vs $\sim 4.9\%$ ID/g spleen). For long-time distribution, we observed that the accumulation of AuNP-C10-SN4 in the liver slightly decreased from 1 d to 7 d and then to 30 d p.i., while that of AuNP-PEG2000 did not change significantly up to 1 month p.i. The accumulation in the spleen changed over time similarly for both AuNPs, which did not change significantly from 1 d to 7 d p.i. but increased at 1 month p.i. Neither mixed-charge nor PEGylated AuNPs exhibited significant change in their total accumulation in the liver and spleen up to 1 month p.i. These results suggest that AuNPs captured by the RES organs are difficult to be clear out, even over long periods of time.^[51,56] Encouragingly, the mixed-charge AuNPs showed excellent ability for minimizing the uptake in the two main RES organs.

For other organs such as the kidney, heart and lungs, we found that the accumulation of AuNP-C10-SN4 was significantly

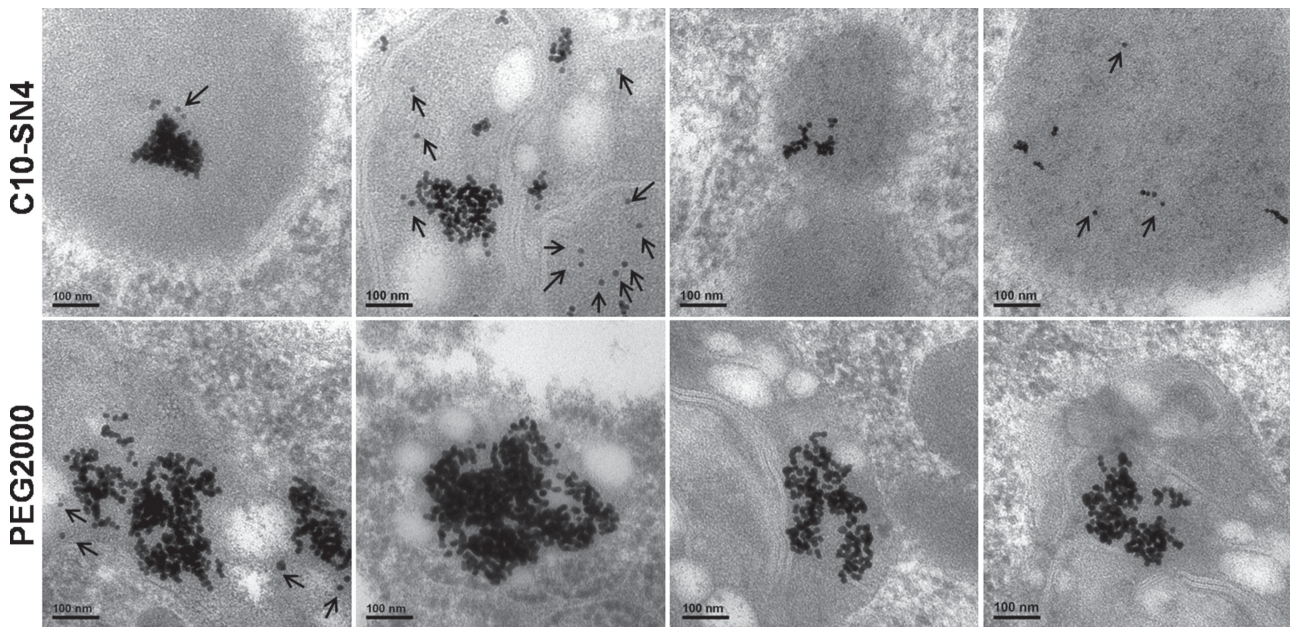


Figure 2. Representative TEM images of liver at 1 month after intravenously injecting AuNP-C10-SN4 (upper) and AuNP-PEG2000 (bottom) in male ICR mice at dose of 100 µg Au per mouse, respectively. Arrows mark the monodispersed AuNPs in cells.

higher than that of AuNP-PEG2000 in all three organs at 24 h p.i. (Figure 1d–f, and given in% ID/g tissue, see Figure S1d–S1f, Supporting Information). Long blood circulation time may partly account for the high content of AuNP-C10-SN4 in these organs at 24 h p.i., when the content of NPs in the blood was still very high (Figure 1a). However, the accumulation of AuNP-C10-SN4 in the kidney decreased to a level similar to that of AuNP-PEG2000 (Figure 1d). The content of AuNP-C10-SN4 in the heart obviously decreased, but was still higher than that of AuNP-PEG2000 as time increased (Figure 1e). Note that the AuNP-C10-SN4 particles have a much longer blood half-life; thus, they have a greater chance to accumulate in the heart, where blood quickly passes through constantly. In contrast, the content of AuNP-C10-SN4 in the lungs was slightly lower than that of AuNP-PEG2000 as time increased (Figure 1f). This behavior can be explained by the concept that AuNP-PEG2000 would more likely be captured by the alveolar macrophages in the lungs. Overall, these results imply that the zwitterionic AuNPs can rapidly distribute into many different organs at 24 h p.i. and that as time increased they would widely spread to other organs or tissues, resulting in a very low content in the heart, kidneys, and lungs.

In order to investigate the possible mechanisms of elimination of zwitterionic NPs, we measured the Au content in urine and feces at times of 0–24 h, 24–48 h, and 48–72 h after a single injection of AuNPs (Figure S3, Supporting Information). The Au content in the urine was extremely low in each measurement; suggesting no obvious clearance of AuNPs through renal excretion. These results are reasonable, as inorganic NPs cleared via the kidney should have a hydrodynamic diameter cutoff of ≈ 6 nm.^[52] The Au content in the feces was higher than that in the urine, but it was still very low and decreased over time. This result indicates that some AuNPs possibly clear through fecal excretion, but for AuNPs this clearance route from body is very

slow. Less than 5% of the injected AuNPs were excreted from the body after injection over the period of 3 d. A thorough examination of long-term excretion of these mixed-charge AuNPs is important and needs further investigation in the future.

2.3. Intracellular Localization of Mixed-Charge AuNPs in the Liver and Spleen

Above results show that the mixed-charge AuNPs accumulated in the liver and spleen far less than did PEG2000 modified ones and most of the AuNPs accumulated in the liver and spleen do not clear out from the body until 1 month p.i. We further used TEM to confirm these results of AuNPs after 1 month p.i. and revealed their cellular distribution and intracellular localization in the liver (Figure 2) and spleen (Figure 3). The mixed-charge AuNP-C10-SN4 were only observed in these phagocytic cells in the liver (detail, see Figure S4, Supporting Information, the cell type in the tissue section can be identified from the morphology of cells in the images with low magnification^[51]) and spleen (detail, see Figure S5, Supporting Information), while no AuNPs were detected by TEM in other cell types. AuNPs were mainly localized in cytoplasmic vesicles, phagosomes, and lysosomes of liver Kupffer cells and spleen macrophages; no uptake occurred in the nuclei, mitochondria, or other special structures. Similar to previous observations of PEG-coated AuNPs,^[51] AuNP-PEG2000 were trapped in liver Kupffer cells (detail, see Figure S6, Supporting Information) and spleen macrophages (detail, see Figure S7, Supporting Information). In contrast, much fewer AuNP-C10-SN4 were found by TEM in both the liver and spleen compared with AuNP-PEG2000; this result agrees with the Au content quantified by ICP-MS.

From the TEM images, most PEGylated AuNPs observed in cells were parts of large aggregates, whereas the mixed-charge

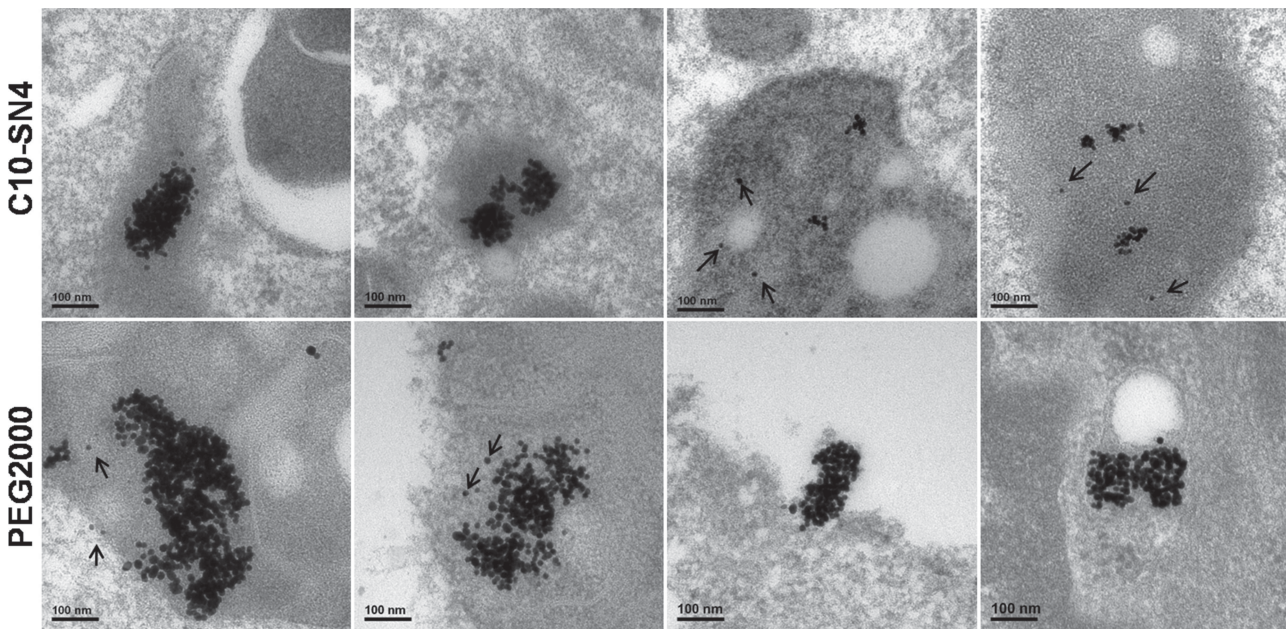


Figure 3. Representative TEM images of spleen at 1 month after intravenously injecting AuNP-C10-SN4 (upper) and AuNP-PEG2000 (bottom) in male ICR mice at dose of 100 µg Au per mouse, respectively. Arrows mark the monodispersed AuNPs in cells.

AuNPs were more likely to exist as parts of small aggregates or individual particles (Figures 2, 3). The single AuNP-C10-SN4 particles observed by TEM suggests that pinocytosis (in addition to phagocytosis) is a mechanism of uptake by phagocytes in the liver and spleen. It has been reported that small clusters in the tumor suggesting tumor cells uptake particles through pinocytosis, while large clusters in the liver suggest that liver cells uptake particles through phagocytosis.^[57,58] Our results show that both AuNPs were taken up by phagocytic cells in the liver and spleen, and many large aggregates were found in phagosomes, which indicate that phagocytosis is one main uptake route.^[51,56,57] Many small clusters and single NPs of AuNP-C10-SN4 were found in lysosomes (a few AuNP-PEG2000 particles and clusters were also observed), suggesting that other pinocytic pathways contribute to the uptake process, one possible pathway being macropinocytosis.^[59] The different states of the two AuNPs within the cells also suggest different endocytic pathways between the mixed-charge and PEGylated AuNPs, but determining the exact mechanism needs extensive investigation in the future. The NPs might also aggregate within cell compartments, where excretion of certain enzymes can induce aggregation of NPs,^[60] which may imply the zwitterionic AuNPs have better in vivo stability than do the PEGylated AuNPs. In addition, the different intracellular states of mixed-charge and PEGylated NPs in immune cells might provide special implications for designing NP-mediated immunotherapy.^[61]

2.4. Biocompatibility of Mixed-Charge AuNPs

When considered as pharmaceutical drugs, NPs should be designed to be eliminated from the body to reduce the potential toxicity induced by accumulation.^[54] However, inorganic are more resistant to elimination routes such as metabolism

and renal excretion because of their large size (too large to be filtered by the kidney) and higher chemical stability (against dissolution and degradation) compared with molecules.^[54] Previous in vitro study has demonstrated that the mixed-charge AuNPs did not cause noticeable cytotoxicity.^[49] In this study, hematoxylin and eosin (H&E) staining revealed no apparent histopathological abnormalities or lesions in the liver, spleen, or kidneys in the AuNP-C10-SN4-treated mice (Figure 4). These results demonstrated that the mixed-charge AuNPs are not notably toxic to the main organs at 1 d, 1 week, or 1 month p.i. at our tested dose (Au: 5 mg kg⁻¹). Moreover, upon injection and throughout the entire study, we observed no unusual behavior or differences between groups of mice, including vocalizations, labored breathing, difficulty moving, hunching, or unusual interactions with cage mates.^[62] We also observed no significant differences in the body weights of mice in all groups throughout the study (Figure S8, Supporting Information). The preliminary low toxicity of these AuNPs evidenced by histological examinations and daily observations suggests that the mixed-charge NPs have good biocompatibility, which is promising for in vivo applications. Biodistribution studies showed that the AuNP-C10-SN4 were widespread in the body, resulting in a low tissue concentration of NPs without the local high accumulation encountered with AuNP-PEG2000 in the liver and spleen; these results suggest a low risk of tissue toxicity for the mixed-charge NPs, as toxicity is related to the localized concentration of NPs.^[56,62]

2.5. Accumulation and Retention of Mixed-Charge AuNPs in Tumors

High accumulation of NPs into tumors is critically important, as it determines the potential efficacy of the NPs for cancer

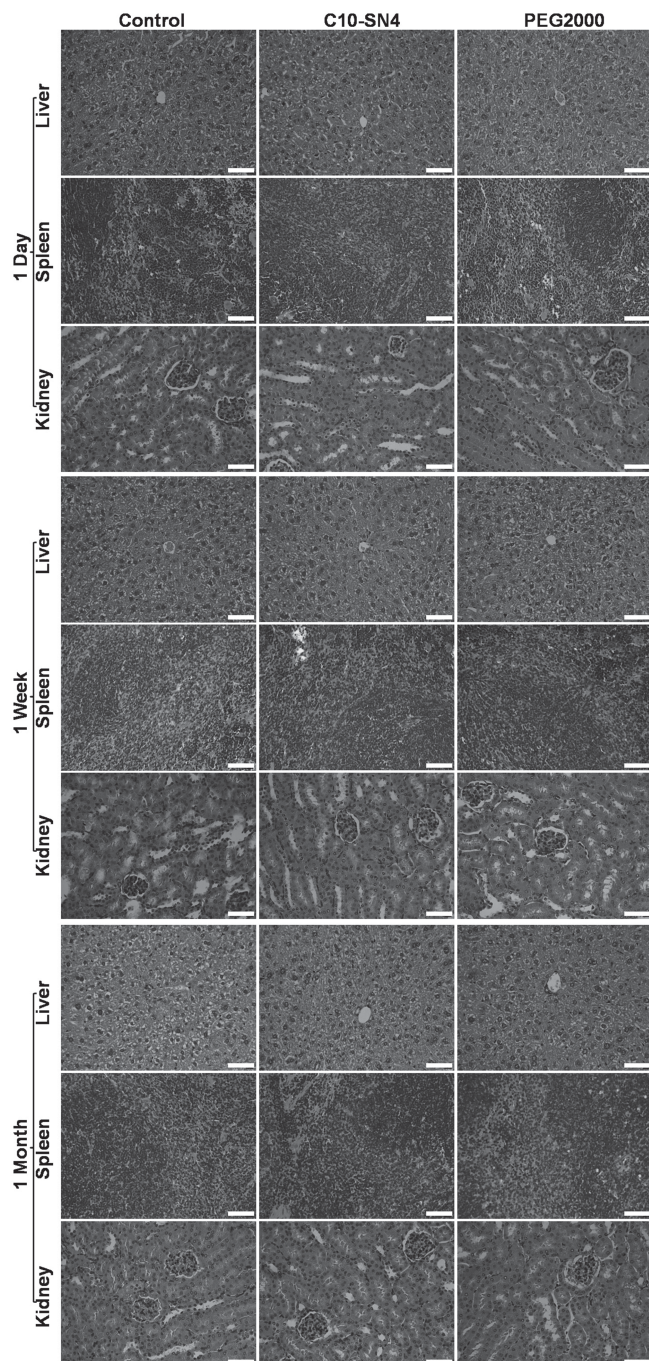


Figure 4. Representative H&E-stained images of major organs including liver, spleen, and kidneys of male ICR mice collected from the control untreated mice, AuNP-C10-SN4 and AuNP-PEG2000 injected mice at various time points p.i. The dose of AuNPs was 100 µg Au per mouse. No notable organ damage or lesion was observed for AuNP-C10-SN4 and AuNP-PEG2000-treated mice. Scale bar is 20 µm.

diagnosis and therapy.^[8,10,12,50,58,63] To establish tumor model, immune-deficient BALB/c nude mice were used in this part. We evaluated the tumor uptake of AuNPs in BALB/c nude mice bearing KB tumors at times of 24 h, 48 h, and 72 h p.i. First, we measured the Au content remaining in the blood; these results showed a similar trend to that in ICR mice (Figure 5a, given

in%ID/g, see Figure S9a, Supporting Information). We found that the tumor uptake of AuNP-C10-SN4 was about twice that of AuNP-PEG2000 at 24 h p.i. (Figure 5b, ≈1.58%ID vs ≈0.87%ID, given in%ID/g, see Figure S9b, Supporting Information). The accumulation of AuNP-C10-SN4 was significantly greater than that of AuNP-PEG2000, but the difference in tumor uptake between the two AuNPs was lower than that in blood. As passive tumor targeting greatly depends on the blood circulation time of NPs, a longer half-life is expected to produce a higher tumor accumulation. Usually, the goal of stealth NPs is to maximize blood circulation half-life to ensure continuous delivery of NPs into the tumor via leaky vasculature. As NPs remain in circulation for longer periods of time, they become more likely to enter the tumor.^[10] However, tumor accumulation is a function of both the rate of extravasation from the blood to the tumor space and the rate of clearance from the tumor. Particles that enter the tumor through leaky vasculature may be carried by convection past the tumor periphery and into the surrounding tissue, where they are likely to be cleared.^[50] Perrault and co-workers^[50] demonstrated that the tumor accumulation of particles in the 20 nm range depends on both size and half-life. This demonstration suggests that the tumor accumulation of AuNP-C10-SN4 is a combined result of AuNPs extravasated from the blood with high NP concentration to the tumor space and of clearing from tumor to periphery tissues at a high rate. We observed that the tumor accumulation of both AuNPs decreased over time (Figure 5b), which indicated gradual clearance of NPs. The retention of AuNP-C10-SN4 was higher than that of AuNP-PEG2000, and the differences between the two AuNPs became more significant as time increased (Figure 5b, ≈1.18%ID vs ≈0.54%ID at 48 h p.i. and ≈1.06%ID vs ≈0.31%ID at 72 h p.i.). When the tumor uptake of AuNPs at different times was normalized to that at 24 h, we clearly observed that the clearance of AuNP-C10-SN4 was much slower than that of AuNP-PEG2000 (Figure 5c, ≈0.67 vs ≈0.35 at 72 h p.i.). Considering that the AuNP-PEG2000 particles being larger than that the AuNP-C10-SN4 particles may have predisposed the retention of PEGylated AuNPs (Figure S2, Supporting Information), we attribute the higher tumor retention of AuNP-C10-SN4 over a long time period to their much longer blood half-life than that of AuNP-PEG2000. The higher retention of these mixed-charge AuNPs in the tumor for longer times resulted in a higher total tumor accumulation, which allows the NPs to interact with the tumor cells for longer periods for a single injection. This result further suggests that a long blood half-life is extremely important for tumor targeting when using small NPs, as their size effect does not favor tumor accumulation because they are able to re-enter the bloodstream and deplete the amount retained within the tumor.^[64]

From this study, the results indicate that surface chemistry plays a significant role in the in vivo behavior of inorganic NPs, the core size of which is already confined as-synthesized. Using mixed-charge zwitterionic surface is a simple strategy for modifying NPs to obtain excellent “stealth” properties in vivo. As the mixed-charge surface endows NPs with strong resistance to plasma protein adsorption, it can greatly delay the opsonization of NPs in blood and reduce their recognition by RES, leading to a long blood circulation time and low accumulation in the liver and spleen. Thus, mixed-charge NPs have many advantages

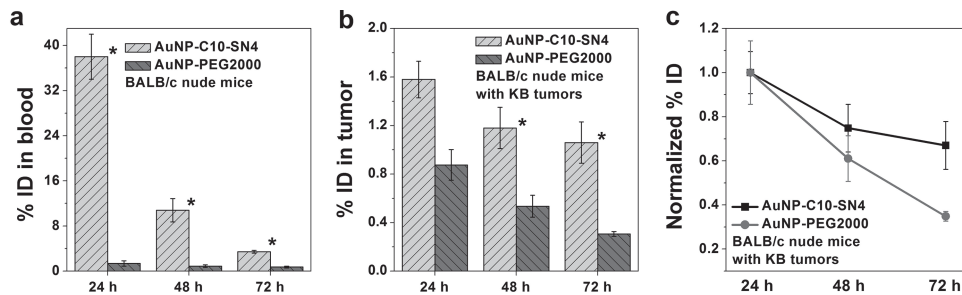


Figure 5. a) Blood retention and b) tumor accumulation of mixed-charge and PEGylated AuNPs in male BALB/c nude mice bearing KB tumors after injecting AuNPs for 24, 48, and 72 h at dose of 100 µg Au per mouse. Each group contained three animals, and results are shown as mean ± S.D, asterisk indicates significant difference, * $p < 0.05$. c) Normalize the tumor uptake at 48 and 72 h p.i. to that at 24 h.

when used as drug carriers or nanodevices for cancer diagnosis and treatment. The longer blood half-life of the NPs gives them more chances to arrive at a desired site such as tumor tissue. When used as drug carriers, the prolonged circulation of NPs allows more drugs to be released at the targeting site, increasing the efficacy of treatment. The low non-specific accumulation in the liver and spleen is greatly beneficial for reducing the side-effects of drugs or background interference of bioimaging NPs in these organs where high accumulation of NPs often occurs. When considering the issue of clearance of NPs from tumor, a long blood circulation becomes dominant when no other factors such as size effects or active ligands favors the retention of NPs in tumor tissues. We believe that tumor uptake can be further enhanced by combining on the surfaces of NPs the excellent “stealth” zwitterionic groups and other active moieties that can respond to the tumor cells or tumor microenvironment. Additionally, the mixed-charge SAMs can effectively stabilize the NPs but do not greatly increase their average size, which is extremely important when designing renally clearable NPs of a small average size to meet the criteria for renal filtration.^[52,53,63]

3. Conclusions

We demonstrated that the mixed-charge AuNPs have promising in vivo behavior for bioapplications. These AuNPs showed excellent stealthy properties in vivo with a long blood half-life of ≈ 30 h and quite low accumulation in the RES organs of less than 10%ID and 1%ID in the liver and spleen, respectively. The mixed quaternary ammonium- and sulfonic-groups-modified AuNPs showed much lower accumulation and different intracellular states in the liver and spleen compared with PEG2000 modified ones. Furthermore, the mixed-charge AuNPs did not cause appreciable toxicity to mice 1 month after a single injection. Importantly, the mixed-charge AuNPs had higher uptake but slower clearance in tumors than did the PEGylated AuNPs because of their prolonged blood half-life. The in vivo results from this work strongly indicates that the mixed-charge strategy can serve as an effective way to design long-circulating, low RES clearance, and high tumor-targeting NPs. These findings in blood circulation, biodistribution, and tumor accumulation of the mixed-charge AuNPs are encouraging to popularize the surface modification of NPs with mixed-charge for biomedical applications.

4. Experimental Section

Gold Nanoparticles Preparation and Characterization: Gold nanoparticles used in this study were prepared by the same way as described previously.^[45] Mixed-charge zwitterionic gold nanoparticles (AuNP-C10-SN4) were synthesized by modifying the 16 nm citrated capped AuNPs with a mixture of negatively charged sodium 10-mercaptopodecanesulfonic acid (HS-C10-S) and positively charged (10-mercaptopodecyl)-trimethyl-ammonium bromide (HS-C10-N4) in 1:1 molar ratio. PEGylated gold nanoparticles (AuNP-PEG2000) were synthesized by modifying the 16 nm citrated capped AuNPs with mercaptopolyethylene glycol ($M_w = 2000$, HS-PEG2000). To minimize the effect caused by ligand density on AuNPs, large excess of ligands (ligand:gold molar ratio of 5) was used in the ligand exchange reaction to make compact coverage of ligands on the AuNP surface. To prepare AuNPs for in vivo tests, both AuNPs were purified by twice centrifugation, and then dispersed in PBS, and filtrated through syringe filters with cellulose acetate membranes with a pore size of 0.45 µm. The hydrodynamic diameter of the AuNPs in physiological PBS and 10% fetal bovine serum (FBS) was measured using dynamic light scattering (DLS). Measurements were performed using a Zetasizer Nano-ZS from Malvern Instruments equipped with a He-Ne laser with a wavelength of 633 nm at 37 °C using a detection angle of 173°. The zeta potential of AuNPs was measured by DLS measurements. The AuNP concentration was analyzed by ICP-MS (Thermo Elemental Corporation of USA, X Series II).

Animals: Animal experiments were performed according to Guidelines for Animal Care and Use Committee, Zhejiang University. Healthy male Institute of Cancer Research (ICR) mice and male BALB/c nude mice were purchased from animal center of Zhejiang Academy of Medical Sciences.

Blood Circulation, Long-Term Biodistribution, and Excretion of AuNPs: Gold nanoparticles given in 0.2 mL PBS with 100 µg Au was injected via the tail vein in each mouse (male ICR mice, 18–22 g). Blood circulation analysis was performed by measuring the remaining gold content from blood taken after injection at different time. Blood samples were collected at 0.5, 3, 6, 12, 24, 48, and 72 h p.i., the total blood weight was estimated to be $\approx 7\%$ of body weight. Long-term biodistribution analysis was performed by measuring the gold content in different tissues after injection for different time. Examined tissues include liver, kidney, spleen, heart, and lung were collected at 1 d, 1 week, and 1 month p.i. For excretion investigation, total urine and feces of mice at times of 0–24 h, 24–48 h, and 48–72 h after injection of AuNPs were collected using metabolism cages. The gold content was analyzed by ICP-MS.

Histological Examinations and Daily Observations: For histology, mice were sacrificed at 1 d, 1 week, and 1 month p.i. and major organs (liver, kidneys, and spleen) were harvested. Organs were fixed in 3.7% neutral buffered formalin, processed routinely into paraffin, sectioned into 4 µm, stained with H&E. The histology was performed in a blinded fashion by professional personnel in the Core Facilities, Zhejiang University School of Medicine. The samples were examined by microscope (Olympus

BX61 Inverted Microscope) in bright-field. Animal behaviors including vocalizations, labored breathing, difficulties moving, hunching, or unusual interactions with cage mates, and body weight were monitored every other day up to 1 month.

Cell Culture and Tumor Xenografts: KB cells (code TCHu 73, human oral epidermoid carcinoma cell line, species of origin: human; tumor type: epithelial cell, source: HeLa contamination) were grown and maintained in RPMI 1640 medium supplemented with 10% FBS, 100 U mL⁻¹ penicillin, and 100 mg mL⁻¹ streptomycin. Cultures were maintained at 37 °C and 5% CO₂ atmosphere. KB cells (2×10^6) in 0.1 mL of PBS were injected subcutaneously into the right rear flank area of male BALB/c nude mice of weight 16 to 18 g. Tumors were allowed to grow to \approx 100 mm³ before experimentation.

Tumor Accumulation and Retention: Nanoparticles given in 0.2 mL PBS with 100 µg Au were injected via the tail vein in each mouse bear KB tumor. Mice were sacrificed at 24, 48, and 72 h p.i. Blood and tumors were collected for measuring the Au content by ICP-MS.

ICP-MS Measurement: Organs and tumors were washed in PBS buffer, and lyophilized for 1 d. Blood was lyophilized directly. The dried tissues and blood were mashed and dissolved in aqua regia for 24 h. Then the aqua regia was diluted and the precipitated tissue debris was removed by centrifugation at 10 000 rpm for 5 min. The Au content in the supernatant was detected by ICP-MS.

TEM Analysis: The liver and the spleen were first fixed in 2.5% glutaraldehyde (in 0.1 M phosphate buffer, pH 7.0). Then, the samples were fixed with 1% osmium tetroxide for 2 h at 4 °C. After being washed in water, the samples were dehydrated in an alcohol series, embedded, and sliced with the thickness between 50 to 70 nm. TEM analysis was performed on a JEM-1230EX TEM operating at 80 kV in a bright-field mode.

Statistic Analysis: All the experiments were repeated at least three times and the data were presented as means \pm standard deviation (SD). The statistical significance was evaluated by the student *t*-test when two groups were compared. In all the tests, the statistical significance was set at *p* < 0.05.

Supporting Information

Supporting Information is available from the Wiley Online Library or from the author.

Acknowledgement

Financial support from the NSFC-21174126, 51333005, National Science Fund for Distinguished Young Scholars (51025312), the National Basic Research Program of China (2011CB606203) and Research Fund for the Doctoral Program of Higher Education of China (20110101110037, 20110101120049, and 20120101130013) and Open Project of State Key Laboratory of Supramolecular Structure and Materials (sklssm201316) are gratefully acknowledged. The authors would like to thank Guping Tang and Jun Zhou for the animal experiment, Ying Xu and Hua Wang for the TEM analysis, and Zigang Xu for the ICP-MS analysis.

Received: November 5, 2013

Revised: January 29, 2014

Published online: February 18, 2014

- [1] M. Ferrari, *Nat. Rev. Cancer* **2005**, *5*, 161.
- [2] D. W. Grainger, D. G. Castner, *Adv. Mater.* **2008**, *20*, 867.
- [3] L. Y. Ang, M. E. Lim, L. C. Ong, Y. Zhang, *Nanomedicine* **2011**, *6*, 1273.
- [4] T. L. Doane, C. Burda, *Chem. Soc. Rev.* **2012**, *41*, 2885.
- [5] E. Boisselier, D. Astruc, *Chem. Soc. Rev.* **2009**, *38*, 1759.

- [6] D. Pissuwan, T. Niidome, M. B. Cortie, *J. Controlled Release* **2011**, *149*, 65.
- [7] Y. C. Yeh, B. Creran, V. M. Rotello, *Nanoscale* **2012**, *4*, 1871.
- [8] R. K. Jain, T. Stylianopoulos, *Nat. Rev. Clin. Oncol.* **2010**, *7*, 653.
- [9] X. Duan, Y. Li, *Small* **2013**, *9*, 1521.
- [10] A. Albanese, P. S. Tang, W. C. W. Chan, *Annu. Rev. Biomed. Eng.* **2012**, *14*, 1.
- [11] S. M. Moghimi, A. C. Hunter, J. C. Murray, *Pharmacol. Rev.* **2001**, *53*, 283.
- [12] S.-D. Li, L. Huang, *Mol. Pharm.* **2008**, *5*, 496.
- [13] D. E. Owens, N. A. Peppas, *Int. J. Pharm.* **2006**, *307*, 93.
- [14] M. A. Dobrovolskaia, P. Aggarwal, J. B. Hall, S. E. McNeil, *Mol. Pharm.* **2008**, *5*, 487.
- [15] R. Gref, A. Domb, P. Quellec, T. Blunk, R. H. Muller, J. M. Veravatz, R. Langer, *Adv. Drug Delivery Rev.* **1995**, *16*, 215.
- [16] G. Storm, S. O. Belliot, T. Daemen, D. D. Lasic, *Adv. Drug Delivery Rev.* **1995**, *17*, 31.
- [17] T. Niidome, M. Yamagata, Y. Okamoto, Y. Akiyama, H. Takahashi, T. Kawano, Y. Katayama, Y. Niidome, *J. Controlled Release* **2006**, *114*, 343.
- [18] D. M. Shin, X. H. Huang, X. H. Peng, Y. Q. Wang, Y. X. Wang, M. A. El-Sayed, S. M. Nie, *ACS Nano* **2010**, *4*, 5887.
- [19] K. Yang, J. Wan, S. Zhang, Y. Zhang, S. T. Lee, Z. Liu, *ACS Nano* **2011**, *5*, 516.
- [20] A. Li, H. P. Luehmann, G. Sun, S. Samarajeewa, J. Zou, S. Zhang, F. Zhang, M. J. Welch, Y. Liu, K. L. Wooley, *ACS Nano* **2012**, *6*, 8970.
- [21] N. J. Ganson, S. J. Kelly, E. Scarlett, J. S. Sundy, M. S. Hershfield, *Arthritis Res. Ther.* **2005**, *8*, R12.
- [22] J. K. Armstrong, G. Hempel, S. Koling, L. S. Chan, T. Fisher, H. J. Meiselman, G. Garratty, *Cancer* **2007**, *110*, 103.
- [23] M. Shen, L. Martinson, M. S. Wagner, D. G. Castner, B. D. Ratner, T. A. Horbett, *J. Biomater. Sci., Polym. Ed.* **2002**, *13*, 367.
- [24] Z. Cao, S. Jiang, *Adv. Mater.* **2010**, *22*, 920.
- [25] Y. Iwasaki, K. Ishihara, *Sci. Technol. Adv. Mater.* **2012**, *13*, 064101.
- [26] Y. Gong, F. M. Winnik, *Nanoscale* **2012**, *4*, 360.
- [27] W. H. Liu, H. S. Choi, J. P. Zimmer, E. Tanaka, J. V. Frangioni, M. Bawendi, *J. Am. Chem. Soc.* **2007**, *129*, 14530.
- [28] L. L. Rouhana, J. A. Jaber, J. B. Schlenoff, *Langmuir* **2007**, *23*, 12799.
- [29] Q. Jin, J. P. Xu, J. Ji, J. C. Shen, *Chem. Commun.* **2008**, 3058.
- [30] V. V. Breus, C. D. Heyes, K. Tron, G. U. Nienhaus, *ACS Nano* **2009**, *3*, 2573.
- [31] W. Yang, L. Zhang, S. L. Wang, A. D. White, S. Y. Jiang, *Biomaterials* **2009**, *30*, 5617.
- [32] E. Muro, T. Pons, N. Lequeux, A. Fragola, N. Sanson, Z. Lenkei, B. Dubertret, *J. Am. Chem. Soc.* **2010**, *132*, 4556.
- [33] J. Park, J. Nam, N. Won, H. Jin, S. Jung, S. Jung, S. H. Cho, S. Kim, *Adv. Funct. Mater.* **2011**, *21*, 1558.
- [34] H. Wei, N. Insin, J. Lee, H. S. Han, J. M. Cordero, W. Liu, M. G. Bawendi, *Nano Lett.* **2011**, *12*, 22.
- [35] X. Chen, J. Lawrence, S. Parelkar, T. Emrick, *Macromolecules* **2013**, *46*, 119.
- [36] D. Kim, M. K. Chae, H. J. Joo, I. Jeong, J. H. Cho, C. Lee, *Langmuir* **2012**, *28*, 9634.
- [37] H. Wei, O. T. Bruns, O. Chen, M. G. Bawendi, *Integr. Biol.* **2013**, *5*, 108.
- [38] R. E. Holmlin, X. X. Chen, R. G. Chapman, S. Takayama, G. M. Whitesides, *Langmuir* **2001**, *17*, 2841.
- [39] S. F. Chen, F. C. Yu, Q. M. Yu, Y. He, S. Y. Jiang, *Langmuir* **2006**, *22*, 8186.
- [40] S. F. Chen, S. Y. Jiang, *Adv. Mater.* **2008**, *20*, 335.
- [41] M. T. Bernards, G. Cheng, Z. Zhang, S. F. Chen, S. Y. Jiang, *Macromolecules* **2008**, *41*, 4216.
- [42] W. Y. Chen, Y. Chang, S. H. Shu, Y. J. Shih, C. W. Chu, R. C. Ruaan, *Langmuir* **2010**, *26*, 3522.

- [43] L. Mi, M. T. Bernards, G. Cheng, Q. M. Yu, S. Y. Jiang, *Biomaterials* **2010**, *31*, 2919.
- [44] X. Peng, L. Zhao, G. Du, X. Wei, J. Guo, X. Wang, G. Guo, Q. Pu, *ACS Appl. Mater. Interfaces* **2013**, *5*, 1017.
- [45] X. S. Liu, H. Y. Huang, Q. Jin, J. Ji, *Langmuir* **2011**, *27*, 5242.
- [46] P. J. BonitatibusJr, A. S. Torres, B. Kandapallil, B. D. Lee, G. D. Goddard, R. E. Colborn, M. E. Marino, *ACS Nano* **2012**, *6*, 6650.
- [47] H. Yang, X. Heng, J. Hu, *RSC Adv.* **2012**, *2*, 12648.
- [48] P. P. Pillai, S. Huda, B. Kowalczyk, B. A. Grzybowski, *J. Am. Chem. Soc.* **2013**, *135*, 6392.
- [49] X. Liu, Q. Jin, Y. Ji, J. Ji, *J. Mater. Chem.* **2012**, *22*, 1916.
- [50] H. C. Fischer, S. D. Perrault, C. Walkey, T. Jennings, W. C. W. Chan, *Nano Lett.* **2009**, *9*, 1909.
- [51] W. S. Cho, M. Cho, J. Jeong, M. Choi, H. Y. Cho, B. S. Han, S. H. Kim, H. O. Kim, Y. T. Lim, B. H. Chung, *Toxicol. Appl. Pharm.* **2009**, *236*, 16.
- [52] H. S. Choi, W. Liu, P. Misra, E. Tanaka, J. P. Zimmer, B. I. Ipe, M. G. Bawendi, J. V. Frangioni, *Nat. Biotechnol.* **2007**, *25*, 1165.
- [53] H. S. Choi, B. I. Ipe, P. Misra, J. H. Lee, M. G. Bawendi, J. V. Frangioni, *Nano Lett.* **2009**, *9*, 2354.
- [54] A. M. Alkilany, C. J. Murphy, *J. Nanopart. Res.* **2010**, *12*, 2313.
- [55] L. Zhang, Z. Cao, Y. Li, J. R. Ella-Menye, T. Bai, S. Jiang, *ACS Nano* **2012**, *6*, 6681.
- [56] W. S. Cho, M. Cho, J. Jeong, M. Choi, B. S. Han, H. S. Shin, J. Hong, B. H. Chung, M. H. Cho, *Toxicol. Appl. Pharm.* **2010**, *245*, 116.
- [57] R. Goel, N. Shah, R. Visaria, G. F. Paciotti, J. C. Bischof, *Nanomedicine* **2009**, *4*, 401.
- [58] J. P. M. Almeida, A. L. Chen, A. Foster, R. Drezek, *Nanomedicine* **2011**, *6*, 815.
- [59] M. Bartneck, H. A. Keul, S. Singh, K. Czaja, J. Bornemann, M. Bockstaller, M. Moeller, G. Zwadlo-Klarwasser, J. Groll, *ACS Nano* **2010**, *4*, 3073.
- [60] T. A. Larson, P. P. Joshi, K. Sokolov, *ACS Nano* **2012**, *6*, 9182.
- [61] D. Boraschi, L. Costantino, P. Italiani, *Nanomedicine* **2012**, *7*, 121.
- [62] M. L. Schipper, N. Nakayama-Ratchford, C. R. Davis, N. W. S. Kam, P. Chu, Z. Liu, X. Sun, H. Dai, S. S. Gambhir, *Nat. Nanotechnol.* **2008**, *3*, 216.
- [63] H. S. Choi, W. Liu, F. Liu, K. Nasr, P. Misra, M. G. Bawendi, J. V. Frangioni, *Nat. Nanotechnol.* **2009**, *5*, 42.
- [64] E. K. Larsen, T. Nielsen, T. Wittenborn, H. Birkedal, T. Vorup-Jensen, M. H. Jakobsen, L. Østergaard, M. R. Horsman, F. Besenbacher, K. A. Howard, *ACS Nano* **2009**, *3*, 1947.